UHASSELT
KNOWLEDGE IN ACTION

Maastricht University

Faculty of Medicine and Life Sciences
School for Life Sciences
Master of Biomedical Sciences

Master's thesis

Cascading Inflammasome Activation: Unravelling its Role in T-Cell Migration across the Blood-Brain Barrier in Multiple Sclerosis Pathogenesis

Joke Aerts

Thesis presented in fulfillment of the requirements for the degree of Master of Biomedical Sciences, specialization Molecular Mechanisms in Health and Disease

SUPERVISOR :

Prof. dr. Bieke BROUX

MENTOR :

Mevrouw Gayel DURAN

2023
2024

Transnational University Limburg is a unique collaboration of two universities in two countries: the University of Hasselt and Maastricht University.

UHASSELT
KNOWLEDGE IN ACTION

www.uhasselt.be
Universiteit Hasselt
Campus Hasselt:
Martelarenlaan 42 | 3500 Hasselt
Campus Diepenbeek:
Agoralaan Gebouw D | 3590 Diepenbeek

UHASSELT
KNOWLEDGE IN ACTION

Maastricht University

Faculty of Medicine and Life Sciences
School for Life Sciences
Master of Biomedical Sciences

Master's thesis

Cascading Inflammasome Activation: Unravelling its Role in T-Cell Migration across the Blood-Brain Barrier in Multiple Sclerosis Pathogenesis

Joke Aerts

Thesis presented in fulfillment of the requirements for the degree of Master of Biomedical Sciences, specialization Molecular Mechanisms in Health and Disease

SUPERVISOR :

Prof. dr. Bieke BROUX

MENTOR :

Mevrouw Gayel DURAN

Cascading Inflammasome Activation: Unravelling its Role in T-Cell Migration across the Blood-Brain Barrier in Multiple Sclerosis Pathogenesis*

Joke Aerts[1], Gayel Duran[1,2], and Bieke Broux[1,2]

[1]Department of Immunology and Infection, Biomedical Research Institute, Universiteit Hasselt, Campus Diepenbeek,
Agoralaan Gebouw C, Diepenbeek, Belgium
[2]University MS Center, Campus Diepenbeek, Diepenbeek, Belgium

*Running title: *Inflammasomes in T-Cell Migration across the BBB*

To whom correspondence should be addressed: Bieke Broux, Tel: +3211269254; Email: bieke.broux@uhasselt.be

Keywords: Inflammasome, T-cells, Multiple sclerosis, Jagged1, Blood-brain barrier

ABSTRACT

Disruption of the blood-brain barrier (BBB) is a crucial aspect of multiple sclerosis (MS), facilitating the migration of myelin-specific T-cells and promoting neuroinflammation. While adaptive immune responses mediated by T-cells are central to MS pathology, the role of innate inflammasomal reactions, particularly in $CD4^+$ T-cells, is increasingly recognised. Inflammasomes are activated via interaction with receptors, such as CD46, that recognise cell damage, microbes, and other ligands like Jagged1, expressed on BBB endothelial cells (ECs). Studies have already explored the connection between inflammasomes in T-cells and the effect of inflammasome activation on T-cell migration across the BBB. Yet, the precise relationship between inflammasome activation and T-cell migration remains elusive.

Here, we investigated whether inflammasome activation precedes or follows T-cell migration using *in vitro* migration assays and co-culture setups. Our findings suggest that T-cell migration across ECs induces inflammasome activation, as evidenced by increased ASC specking in $CD4^+$ T-cells. However, IL-1β was also increased when $CD4^+$ T-cells only had contact with inflamed ECs, suggesting that contact with inflamed ECs is also sufficient to activate the inflammasome. Furthermore, inflammasome activation exacerbates disease severity, as demonstrated in experimental autoimmune encephalomyelitis models. Knockout mice for inflammasome activation exhibited a decrease in Th1/Th17 ratio in the lymph nodes of NLRP3 KO mice, indicating the critical role of inflammasomes in Th17 cell migration.

Collectively, these findings demonstrate that T-cell migration across the BBB triggers inflammasome activation within these cells and aggravates MS severity. Targeting the inflammasome may, therefore, offer novel therapeutic approaches for MS, meriting further research.

INTRODUCTION

Multiple Sclerosis (MS) is an incurable neurodegenerative autoimmune disease that affects around three million people worldwide (1). It is characterised by an auto-immune attack against the central nervous system (CNS) by myelin-specific T-cells (2). Due to inflammatory mediators released by immune cells, the blood-brain barrier (BBB), protecting the CNS, becomes disrupted, making it susceptible to further immune cell infiltration (2). This will eventually result in chronic inflammation, demyelination, and neuronal loss (2, 3). MS presents in three distinct forms: Primary Progressive Multiple Sclerosis (PPMS) is a form of MS that exhibits gradual deterioration from the onset, resulting in the accumulation of disabilities, such as muscle weakness and ataxia, without any periods of symptom improvement (2, 3). In contrast, Relapsing-Remitting Multiple Sclerosis (RRMS) is characterised by periods of symptom

relapses caused by neuroinflammation due to T- and B-cell infiltration across the compromised BBB into the CNS. These relapses alternate with recovery phases that last weeks or months (2, 3). As RRMS progresses, it often transitions into Secondary Progressive Multiple Sclerosis (SPMS), which is marked by a gradual decline in neurological function due to demyelination rather than neuroinflammation (2).

Since neuroinflammation is a key characteristic of early RRMS phases, the role of adaptive immune cells, particularly T-cells and auto-antigens, is a central aspect of MS pathogenesis (2, 4, 5). However, neuroinflammation in MS extends beyond the adaptive immune system to include components of the innate immune system, such as inflammasomes that can be activated in T-cells (5-7).

These multiprotein complexes assemble in the cytosol of injured or pathogen-inflicted cells and are not confined to a single epitope (8). Inflammasomes consist of oligomers formed by a sensor molecule, such as NOD-like receptor protein 3 (NLRP3), caspase-1, and the adaptor Apoptosis-associated Speck-like protein containing a Caspase recruitment domain (ASC), which links these two components together (8, 9). The activation of these complexes leads to the activation of caspase-1, resulting in the subsequent cleavage of pro-interleukin (IL)-1β and pro-IL-18 into their biologically active forms. In addition to these cytokines, caspase-1 also cleaves gasdermin D (GSDMD), which then oligomerises and assembles into a plasma membrane channel that releases IL- 1β and IL-18 and allows an influx of ions followed by pyroptosis (8, 9).

In addition to the production of interleukins and GSDMD, the inflammasome has also been the focus of previous research linking components of the adaptive and innate immune system. This has indicated that the NLRP3 inflammasome is an important regulator of type 1 and 17 T helper (Th1 and Th17) cell responses in the development of experimental autoimmune encephalomyelitis (EAE), a mouse MS model (10). Furthermore, studies have outlined both the extrinsic inflammasome activation and intrinsic inflammasome activation in $CD4^+$ T-cells to be involved in the differentiation into Th1 and Th17 cells (4, 10-12). Given that Th1 and Th17 cells play a pivotal role in disrupting the BBB in MS and inducing neuroinflammation upon migration into the CNS, understanding the regulation of T-cell activation and differentiation is of significant importance (2, 4). Moreover, additional studies have supported the link between inflammasomes and T-cells by demonstrating that inflammasome activation is not restricted to damaged or pathogen-affected cells as part of the innate immune response only; it also occurs, for example, when CD46, a T-cell receptor, is activated (7). In addition to various human pathogens (6), Jagged1 (Jag1) is also identified as a ligand of CD46 and is particularly interesting due to its high expression on the BBB-endothelial cells (ECs) (6, 7, 13). Furthermore, a study by Inoue *et al.* (2012) concluded that NLRP3 inflammasome activation is indispensable for the migration of $CD4^+$ T-cells across the BBB and their entry into the CNS. Additionally, this study observed a notable increase in Th17 cells within the lymph nodes compared to Th1 cells on day nine post-EAE induction (onset of EAE) (14). The reason for this imbalance between Th cell subsets remains currently unknown. Another study by Martin *et al.* (2016) demonstrated that T-cell-intrinsic ASC is required for Th17-mediated EAE, as this study found that ASC deficiency in T-cells impaired Th17 cell-mediated but not Th1 cell-mediated EAE (12). Moreover, the precise relationship between T-cell intrinsic inflammasome activation and their migration over the BBB remains elusive, as it is unclear whether inflammasome activation is necessary for T-cell migration or if it is a consequence of it. Additionally, it is uncertain whether direct contact between T-cells and endothelial cells alone results in inflammasome activation or if this activation is specifically induced by the process of T-cell migration across ECs (12, 14). Furthermore, the impact of inflammasome activation within T-cells on the pathogenesis of EAE and MS remains limitedly investigated (4, 14). However, preliminary data indicate that $CD4^+$ T-cell inflammasome activation increases in the CNS compared to the lymph nodes and spleen when EAE was induced in mice with a GFP-labelled ASC protein (data not shown).

Given that T-cells play a significant role in disrupting the BBB in MS and causing neuroinflammation upon reaching the CNS, the main challenges lie in an incomplete understanding of the specific mechanisms driving inflammasome

activation in T-cells, which, in turn, can contribute to BBB disruption and exacerbate neurodegeneration after crossing the BBB.

In light of this, we aimed to investigate which molecular trigger activates the inflammasome in T-cells *in vitro*, as well as its necessity to cross the BBB *in vivo* and thus plays a significant role in the development of MS. We hypothesise that Jag1 is the molecular trigger for inflammasome activation necessary in T-cells to cross the BBB *in vitro* and *in vivo* and thereby plays a role in the pathophysiologic mechanisms of MS.

To test this hypothesis, we studied the effect of inflammasome activation in MS pathology *in vivo* by inducing EAE in wild-type (WT) and NLRP3 knockout (KO) mice. We provide evidence that NLRP3 KO mice experience less severe disease development and a decrease in Th1/Th17 ratio in the lymph nodes of NLRP3 KO mice, indicating the critical role of inflammasomes in Th17 cell migration. Moreover, we investigated whether inflammasome activation is necessary for T-cell migration *in vitro* or whether it results from migration. We report that the actual T-cell migration process over inflamed ECs increases inflammasome activation in $CD4^+$ T-cells, suggesting that $CD4^+$ T-cell migration induces inflammasome activation. Furthermore, we found that direct contact between $CD4^+$ T-cells and inflamed ECs also enhances IL-1β production. In addition, we measured the expression levels of Jag1 in resting and inflamed BBB cells *in vitro*, demonstrating that inflammation increases Jag1 expression in brain ECs. Finally, we confirmed the presence of Jag1 in the brains of human MS patients and EAE mice, along with ASC in the EAE mice.

Together, these findings highlight that T-cell migration across the BBB triggers inflammasome activation within these cells and aggravates MS severity. These insights enhance the understanding of inflammasome activation in T-cells and ultimately contribute to unravelling the MS pathophysiology.

EXPERIMENTAL PROCEDURES

Mice – NLRP3-knockout mice (B6.129S6-Nlrp3tm1Bhk/J, strain#:021302, The Jackson Laboratory), their respective wild-type (WT) mice (C57BL/6J, strain #: 000664, The Jackson Laboratory), and mice with green fluorescent protein (GFP)-labelled ASC proteins (ASC-GFP mice, B6.Cg-Gt(ROSA)26Sortm1.1(CAG-Pycard/mCitrine*,-CD2*)Dtg/J, strain#:030744, The Jackson Laboratory) were bred and housed on a 12-hour light/dark cycle with *ad libitum* access to water and a standard chow diet. All animal procedures were conducted in accordance with the institutional guidelines and approved by the Ethical Committee for Animal Experiments of Hasselt University.

EAE induction – 11-week-old female WT ($n = 5$) and NLRP3 KO ($n = 5$) mice were subcutaneously injected with myelin oligodendrocyte glycoprotein (MOG)35–55 emulsified in complete Freund's adjuvant (CFA) containing Mycobacterium tuberculosis (Hooke Laboratories). Immediately after and the next day after immunisation, mice were injected intraperitoneally (i.p.) with 110 ng/100 µl pertussis toxin (PTX). Daily monitoring of weight and neurological deficits was performed using a 5-point scale (0: no symptoms; 1: limp tail; 2: weakness of hind legs; 3: complete paralysis of hind legs; 4: complete hind and partial front leg paralysis; 5: death). To evaluate the immune cell profile by flow cytometry, immune cells were isolated from the halve of the CNS, draining lymph nodes and spleen at EAE onset (13 dpi) (as described in (15-18)) and stained for CD45 Alexa Fluor 700, CD3 FITC, CD4 Pacific Blue, CD8a Brilliant Violet 510, CD19 Brilliant Violet 650, CD11b PERCP/Cy5.5, Ly6C Brilliant Violet 785, IL-4 PE, IL-17 PE/Dazzle 594, IFNγ PE-Cy7, and Foxp3 Alexa Fluor 647 (all BioLegend. The other half of the brain and spinal cord was frozen and kept for IHC.

Cell culture – All cells were cultured at 37°C/5% CO_2.

Primary mouse brain microvascular endothelial cells: isolation and culturing – Primary mouse brain microvascular endothelial cells (mBMECs) were isolated from 4- to 6-week-old WT and ASC-GFP mice as described previously (15). Briefly, brains were dissected, and meninges and choroid plexuses were removed. Remaining parenchymal brain tissue was minced, homogenised, and digested with DMEM containing 0.7 mg/ml collagenase type II (Gibco™, Thermo Fisher Scientific) and 39 U/ml DNase. Myelin was removed by centrifugation at 1000 g in 20% bovine serum albumin (BSA, Merck) in DMEM. The remaining pellet was further digested with 1 mg/ml collagenase/dispase (Roche Diagnostics GmbH)

and 39 U/ml Dnase I in DMEM. Brain microvessels were obtained using a 33% continuous Percoll gradient. The resulting primary ECs were plated in 10 µg/ml collagen type IV (Merck)-coated well plates. mBMECs were cultured in DMEM supplemented with 20% foetal calf serum (FCS, Biowest), 1 ng/ml FGF, 100 µg/ml heparin, 1.4 µM hydrocortisone (all Merck) and 0.5% penicillin/streptomycin antibiotic–antimycotic solution. The first 48h cells were grown in medium containing 10 µg/ml puromycin (Sigma-Aldrich) to obtain pure EC cultures. After, puromycin concentration was decreased to 4 µg/ml for 24h. After that, cells were cultured in medium without additional puromycin. Inflammation was induced by treatment with 10 ng/ml rmTNFα and 10 ng/ml rmIFNγ (both Peprotech) for 24h (qPCR) or 48h (ICC).

Human brain-derived endothelial cells – The human cerebral microvascular endothelial cell line hCMEC/d3 was provided by Tebu-bio (Le Perray-en-Yvelines) and cultured as previously described (15, 16). Inflammation was induced by treatment with 100 ng/ml rhTNFα and 10 ng/ml rhIFNγ (Peprotech) for 24h.

Mouse brain-derived endothelial cells – The mouse brain endothelial cell line mBEND3 was provided by American Type Culture Collection (CRL-2299™) and cultured in DMEM (41966029, Gibco™, Thermo Fisher Scientific) supplemented with 10% FCS (Biowest). Inflammation was induced by treating the cells with 150 ng/ml rmTNFα and rmIFNγ (both Peprotech) for 24h.

Migration assay – hCMEC/d3 cells were spilt on inserts and cultured, and inflammation was induced by treatment with 100 ng/ml rhTNFα and 10 ng/ml rhIFNγ for 24h. Peripheral blood mononuclear cells (PBMCs) were isolated from whole blood of healthy donors (Table S1) using density gradient centrifugation (Ficoll-Paque™ PLUS, GE Healthcare) and were added to the inserts, with or without 45µM MCC950 (an inflammasome inhibitor, 5.38120, Merck) to inhibit NLRP3 inflammasome activation. After 24h, the migrated and non-migrated cells were collected and analysed with flow cytometry.

Co-culture – mBEND3 and hCMEC/d3 cells were cultured until confluency in a 6-well plate. Inflammation was induced by treating the cells with TNFα and IFNγ for 24h, as described above. Resting endothelial cells served as a control and were cultured in medium without cytokine treatment. After 24h treatment, mouse $CD4^+$ T-cells were isolated from the spleens of ASC-GFP mice with the EasySep™ Mouse $CD4^+$ T-cell isolation kit (19852, STEMCELL Technologies), following the manufacturer's instructions. Spleens were isolated as described before (15, 16). Briefly, cell suspensions were derived, and the splenocytes were lysed with 0.83% ammonium chloride and cultured. Human $CD4^+$ T-cells were isolated from PBMCs using the human Memory $CD4^+$ T-Cell Isolation Kit (130-091-893, Miltenyi Biotec), following the manufacturer's instructions. The $CD4^+$ T-cells were or were not treated with 10 µM nigericin (an inflammasome activator, SML1779, Merck) for 30 minutes. The $CD4^+$ T-cells were added to the endothelial cells to create a co-culture. After 24 hours, all cells were collected for analysis.

Flow cytometry – Zombie NIR (BioLegend) and fixable viability dye eFluor™ 506 (eBioscience™) were used as live/dead staining. To determine the different immune cell populations, cells were stained for intra- and extracellular markers (Table S2). The cells were incubated for extracellular markers for 30 minutes; whereafter they were permeabilised with the Foxp3/Transcription Factor Staining Buffer Set (00-5523-00, eBioscience™) for one hour and stained for intracellular markers for 30 minutes. The BD-LSRFortessa flow cytometer (BD Biosciences) with FACSDiva software (BD Biosciences) or the Aurora Cytek spectral flow cytometer (Cytek Biosciences) with SpectroFlo software (Cytek Biosciences) were used to quantify cellular fluorescence, and data were analysed with FlowJo software (BD Bioscience) version 10.8.1.

Enzyme-linked immunosorbent assay – Conditioned medium of the human co-culture was collected after 24h. IL-1β was analysed using the ELISA MAX™ Deluxe Set Human IL-1β (437004, BioLegend) according to manufacturer's instructions. Absorbance was measured at 450 nm using a Tecan plate reader.

Immunohistochemistry – *Post-mortem* human brain sections (n = 1 MS patient, four coupes) were fixed in frozen acetone and blocked with 50% Dako® protein block in PBS/0.05% Tween20 for 30 minutes at room temperature. Next, sections were incubated with rabbit-anti-jagged1 (1:100, PA5-86057, Invitrogen) or mouse-anti-IL-1β (1:100, sc-32294, SantaCruz Biotechnology) as primary

antibodies at 4 °C overnight. Immunoreactivity was visualised using goat anti-rabbit Alexa Fluor 555 (1/250) and goat anti-mouse Alexa Fluor 555 (both Invitrogen™, Thermo Fisher Scientific) after 1h incubation at room temperature. Nuclear staining was performed with 4',6-diamidino 2-phenylindole (DAPI). Finally, sections were incubated with 0.3% Sudan Black (Merck) in 70% ethanol to limit autofluorescence and mounted with Fluoromount-G™ Mounting Medium (Invitrogen™, Thermo Fisher Scientific). Microscopic analysis was performed using Leica DM2000 LED and Leica Application Suite X (LAS X) software (Leica Microsystems).

Immunocytochemistry – mBMECs were fixated in 4% paraformaldehyde for 30 minutes and blocked with 10% Dako® protein block in PBS. Next, sections were incubated with rabbit-anti-jagged1 (1:100, PA5-86057, Invitrogen) at 4 °C overnight. Immunoreactivity was visualised using goat anti-rabbit Alexa Fluor 555 (1/250; Invitrogen™, Thermo Fisher Scientific) after 1h incubation at room temperature. Nuclear staining was performed with 4',6-diamidino 2-phenylindole (DAPI). Microscopic analysis was performed as described above.

Statistical analysis – Data were statistically analysed using GraphPad Prism v10 (GraphPad Software Inc.) and are reported as mean ± S.E.M. The Shapiro-Wilk normality test was used to test for normal distribution. When the datasets were normally distributed, a one-way ANOVA (Tukey's *post hoc* analysis), a two-way ANOVA (Bonferroni's *post hoc* analysis), a two-tailed unpaired Student's t-test (with Welch's correction if necessary), or a Pearson r correlation test was used to determine statistical significance between groups. When datasets are not normally distributed, a Kruskal-Wallis test (Dunn's *post hoc* analysis), a Wilcoxon rank sum analysis, or a Spearman r correlation test was performed. P-values < 0.05 were considered to indicate a significant difference between the groups (*, $p < 0.05$; **, $p < 0.01$; ***, $p < 0.001$; ****, $p < 0.0001$).

RESULTS

NLRP3 knock-out decreases EAE disease severity and Th17 cell migration – Given previous research suggesting the involvement of T-cell inflammasome activation in T-cell migration in EAE (14), we aimed to validate this phenomenon *in vivo*. To this end, we induced EAE in NLRP3 KO mice with no inflammasome activation via NLRP3. Notably, these mice exhibited significantly less severe EAE symptoms compared to WT mice, as indicated by reduced weight loss and a lower sum of EAE scores (Fig. 1A-C). The immune cell profile in draining lymph nodes, spleen and CNS was analysed at disease onset using flow cytometry. There were significantly more Th1 cells compared to Th17 cells in all three organs (Fig. 1D-F). While there were no significant differences in the spleen and CNS (Fig. 1D-E), Th1 and Th17 cells tended to be more prevalent in the CNS of WT mice (Fig. 1D). Conversely, Th1 and Th17 cells were significantly more abundant in the lymph nodes of NLRP3 KO mice compared to WT mice (Fig. 1F). Additionally, when comparing Th1/Th17 ratios across the three organs, the ratio was significantly decreased in the lymph nodes of NLRP3 KO mice (Fig. 1I). The Th1/Th17 ratio also appeared to decrease in the spleens of NLRP3 KO mice and seemed to increase in the CNS of NLRP3 KO mice compared to WT mice (Fig. 1G-H), indicating that especially the Th17 cells could not migrate into the CNS.

Overall, these findings strongly support the notion that the inflammasome contributes to EAE pathogenesis, potentially through its influence on Th17 cell migration.

Migration of human PBMCs cells through inflamed endothelial cells increases ASC specking in $CD4^+$ T-cells – Considering that our *in vivo* studies supported the role of inflammasome activation in T-cell migration, we aimed to further investigate this T-cell migration process through ECs and the specific role of inflammasome activation. To explore this, an *in vitro* migration assay was conducted using human PBMCs and hCMEC/d3 cells to model the BBB. First, it was assessed whether inflammasome activity influenced migration. Treatment of PBMCs with the inflammasome inhibitor MCC950 resulted in a slight decrease in the percentage of migrated cells (Fig. 2A-B) and significantly reduced the total percentage of ASC speck formation (Fig. 2C). Further analysis revealed a significant increase in ASC specking in migrated $CD4^+$ T-cells compared to non-migrated cells, which was diminished with MCC950 treatment (Fig. 2D). Similar patterns were observed in $CD8^+$ T-cells, classical monocytes, and

B-cells (Fig. 2E-H). However, in non-classical monocytes, ASC speck formation displayed an opposing trend (Fig. 2G).

These findings suggest that the migration of $CD4^+$ T-cells across the BBB enhances inflammasome activation in these immune cells.

Contact of human $CD4^+$ T-cells with inflamed endothelial cells increases IL-1β production – Given that the migration of $CD4^+$ T-cells across ECs enhances inflammasome activation, a co-culture experiment was designed to assess whether direct contact between ECs and T-cells alone could induce this inflammasome response. In this experiment, inflamed or resting hCMEC/d3 cells were co-cultured for 24h with $CD4^+$ memory T-cells treated with or without the inflammasome activator nigericin. Results indicated that contact between $CD4^+$ T-cells and ECs did not affect ASC specking in any of the Th subsets (Fig. 3A-F). Moreover, it was also investigated whether inflammasome activation resulted in more Th17 cells compared to regulatory T-cells (Treg). However, analysis showed that nigericin-treated T-cells in contact with inflamed ECs decreased the number of Tregs, diminishing the significant difference between Tregs and Th17 seen in other conditions (Fig. S1). Additionally, inflammation did not significantly impact the expression of Jag1 (Fig. 3H), nor did it affect the ICAM, VCAM, or VE-cadherin expression in hCMEC/d3 cells (Fig. S2).

To provide a more complete picture of inflammasome activation, IL-1β concentrations in the co-culture supernatant were determined. Results revealed that inflamed ECs co-cultured with nigericin-treated $CD4^+$ memory T-cells significantly increased IL-1β production (Fig. 3G), indicating that inflammasome activation in $CD4^+$ T-cells, together with inflamed ECs, leads to a significant increase in IL-1β production.

However, when this experiment was conducted using mBEND3 cells and mouse $CD4^+$ splenocytes, nigericin-treated Th1 cells co-cultured with inflamed ECs exhibited significantly reduced ASC speck formation compared to resting Th1 cells with control ECs (Fig. 4A). Additionally, resting Th17 co-cultured with control ECs showed significantly higher ASC specking compared to Th17 cells without EC contact (Fig. 4B). This pattern was also observed in the ASC mean fluorescence intensity across all $CD4^+$ T-cells (Fig. 4D). No difference was observed in Treg cells (Fig. 4C). Furthermore, Jag1 expression in mBEND3 cells remained unchanged (Fig. 4E).

Overall, these results indicate that dual inflammasome activation in human $CD4^+$ T-cells, along with contact with inflamed ECs, boosts IL-1β production. Conversely, inflamed ECs reduce inflammasome activation in mouse $CD4^+$ T-cells.

Inflammation increases Jag1 expression in brain endothelial cells – Considering that the co-culture studies revealed increased IL-1β production upon direct contact between $CD4^+$ T-cells and inflamed ECs, it was investigated whether Jag1 could be the responsible trigger. To explore this, ECs were treated with TNFα and IFNγ for 24h or 48h to model inflammation. Jag1 expression was quantified at gene level via qPCR and protein level using ICC. Analysis demonstrated a significant increase in Jag1 expression in inflamed mBEND3 cells (Fig. 5A). Although hCMEC/d3 and mBMECs also displayed elevated Jag1 expression following inflammation, these increases were not statistically significant ($p = 0.0622$ and $p = 0.7321$, respectively; Fig. 5B-C). Protein-level validation on mBMECs supported these trends of increased Jag1 expression (Fig. 5D, F). ASC expression was also assessed at protein level and increased significantly with inflammation (Fig. 5D-E).

These findings collectively suggest that inflammation in BBB ECs is associated with upregulated Jag1 expression, potentially contributing to $CD4^+$ T-cell inflammasome activation upon contact with and migration through ECs.

ASC and Jag1 are expressed in the CNS of MS patients and EAE mice – In light of the suggested role of EC inflammation in Jag1 expression and $CD4^+$ T-cell inflammasome activation, the potential involvement of Jag1 in MS pathogenesis was investigated. To explore whether Jag1 could be the missing link between inflamed ECs and $CD4^+$ T-cell inflammasome activation, we first assessed the presence of Jag1 in the brains of MS patients. Immunostaining of active human MS lesions revealed distinct Jag1 expression, mainly concentrated around blood vessels (Fig. 6A-B). Similarly, in ASC-GFP mice induced with EAE, concurrent expression of ASC and Jag1 was

observed at the disease peak in both brain and spinal cord tissues. However, no significant correlation was found (Fig. 6C-F). Notably, the ASC signal predominantly localised around the choroid plexus and blood vessels in the brain, while in the spinal cord, both ASC and Jag1 signals were notably enhanced at tissue margins.

Additionally, immunostaining for IL-1β was performed to provide a complete assessment of inflammasome activation. IL-1β expression was evident in active human lesions (Fig. S3). However, it should be noted that further protocol optimisation is required.

These findings collectively confirm the presence of Jag1 and IL-1β within the CNS of MS patients, and Jag1 and ASC in the CNS of EAE mice, suggesting the active involvement of the inflammasome in facilitating immune cell infiltration into the CNS.

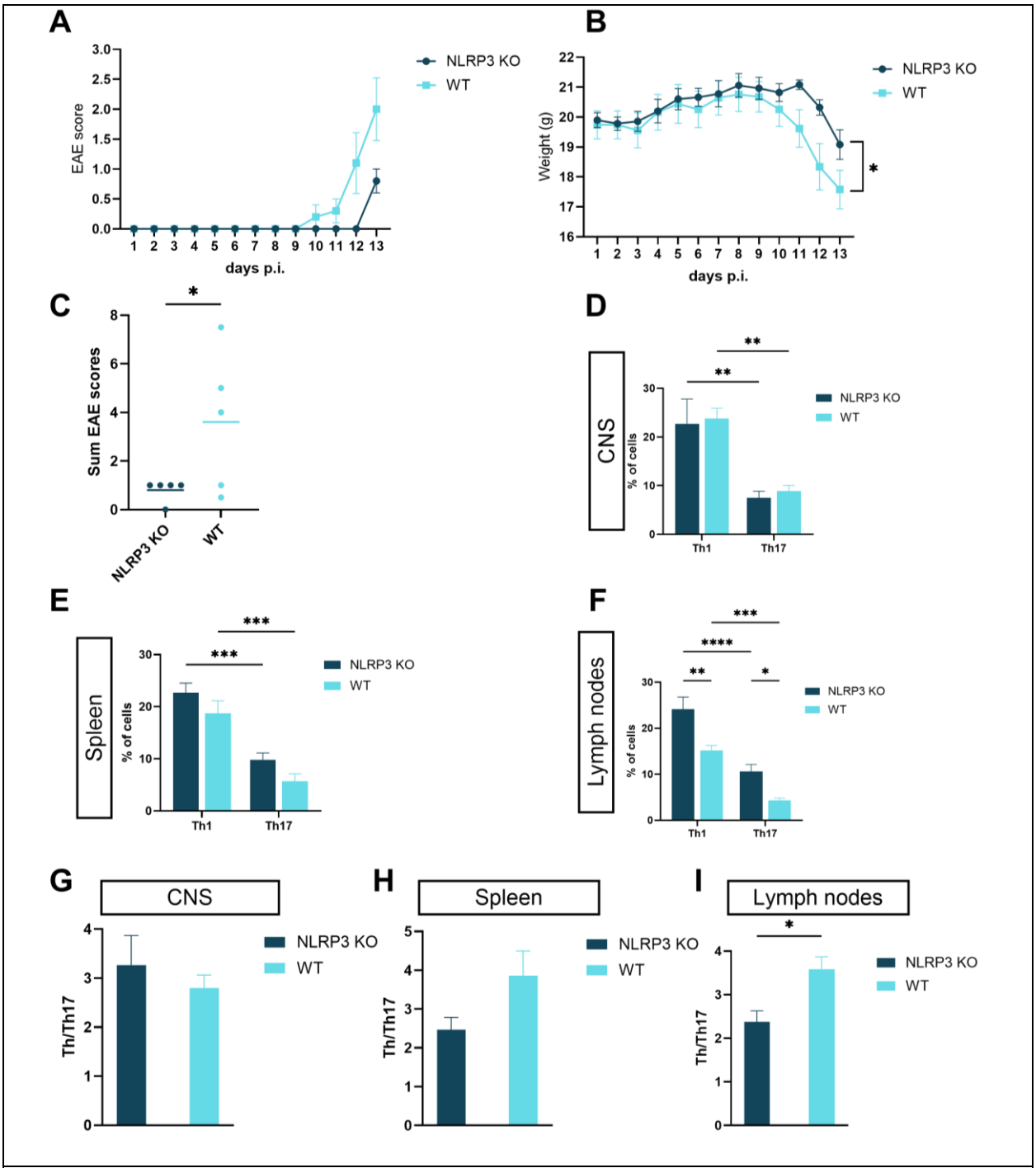

Fig. 1: NLRP3 knock-out decreases EAE disease severity. (A) Daily clinical scores and **(B)** weights were measured. **(C)** The sum of EAE scores was analysed (n = 5 per group). Mice were sacrificed at onset (13 days p.i.) **(D-F)** Flow cytometric analysis of the percentage of Th1 and Th17 cells in the CNS **(D)**, spleen **(E)**, and lymph nodes **(F)** in NLRP3 KO and WT mice. The ratio of Th1 and Th17 cells in the CNS **(G)**, spleen **(H)**, and lymph nodes **(I)** in NLRP3 KO and WT mice. Statistical analysis was performed using a Mann-Whitney test (A, G-I), an unpaired t-test (B-C), and a two-way ANOVA with a Bonferroni's multiple comparisons test (D-F) with *, $p < 0.05$; **, $p < 0.01$; ***, $p < 0.001$; ****, $p < 0.0001$. Data are depicted as mean ± SEM. *NLRP3, NOD-like receptor protein 3; WT, wild-type; p.i., post-immunisation; EAE, experimental autoimmune encephalomyelitis; CNS, central nervous system.*

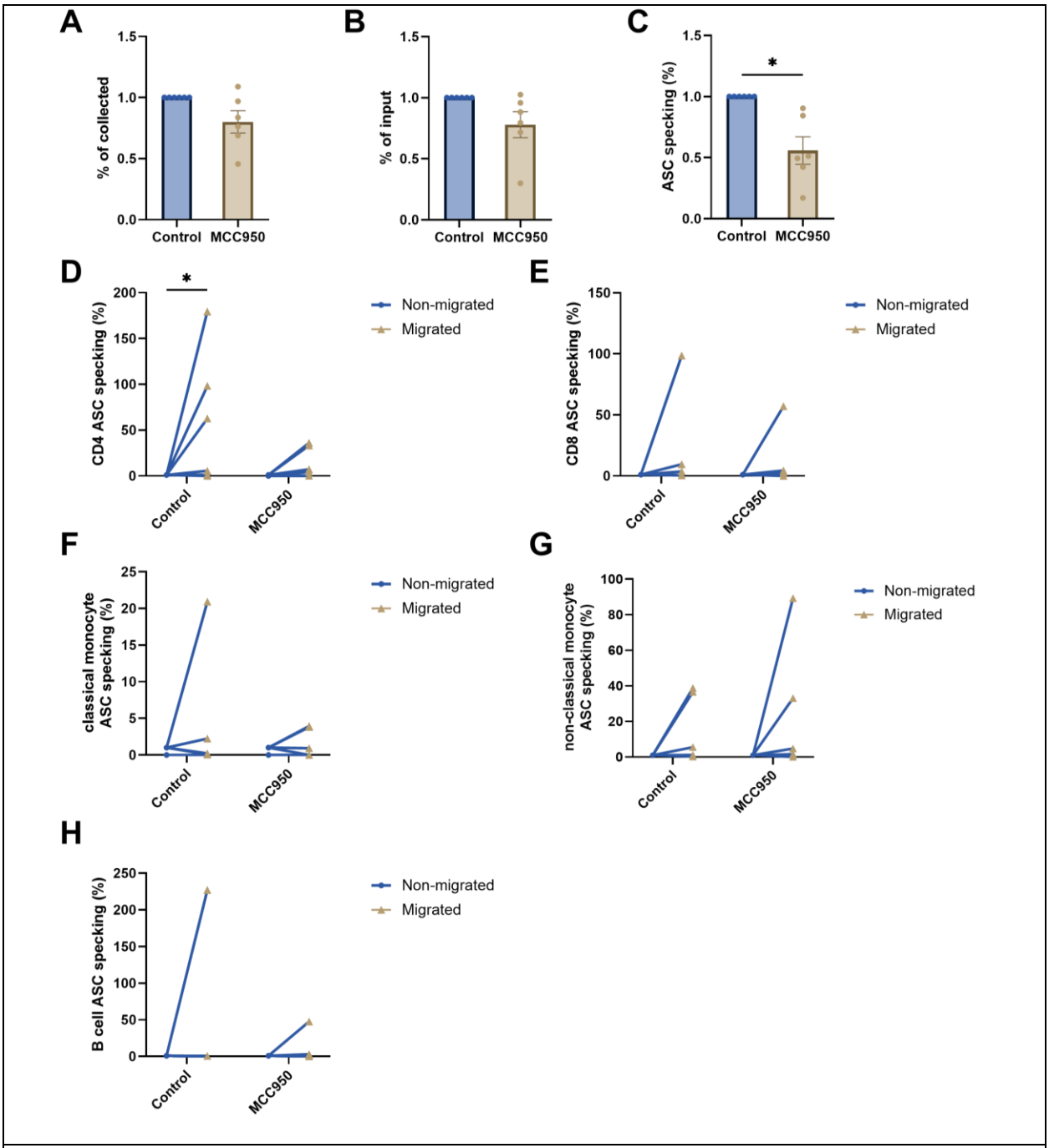

Fig. 2: Migration of human PBMCs through endothelial cells increases ASC specking in CD4$^+$ T-cells. (A) Relative percentage of PBMCs found in bottom compartment after 24h as a percentage of total plated cells. **(B)** Relative percentage of cells found in bottom compartment after 24h as a percentage of PBMCs found (top + bottom). **(C-H)** Relative percentage of ASC specking was analysed using flow cytometric analysis in all cells in total **(C)** CD4$^+$ T-cells **(D)**, CD8$^+$ T-cells **(E)**, classical monocytes **(F)**, non-classical monocytes **(G)**, and B cells **(H)** (n = 6). PBMCs were untreated or treated with MCC950, and hCMEC/d3 cells were untreated or treated with TNFα and IFNγ for 24h. Data is from six different HDs, and statistical analysis is done using a paired t-test (A-B) and a two-way ANOVA with a Bonferroni's multiple comparisons test (D-H) with *, p<0,05. Data are depicted as mean ± SEM. *ASC, Apoptosis-associated Speck-like protein containing a Caspase recruitment domain; PBMCs, Peripheral Blood Mononuclear Cells; TNFα, tumour necrosis factor alpha; IFNγ, interferon gamma; IL-1β, interleukin-1β.*

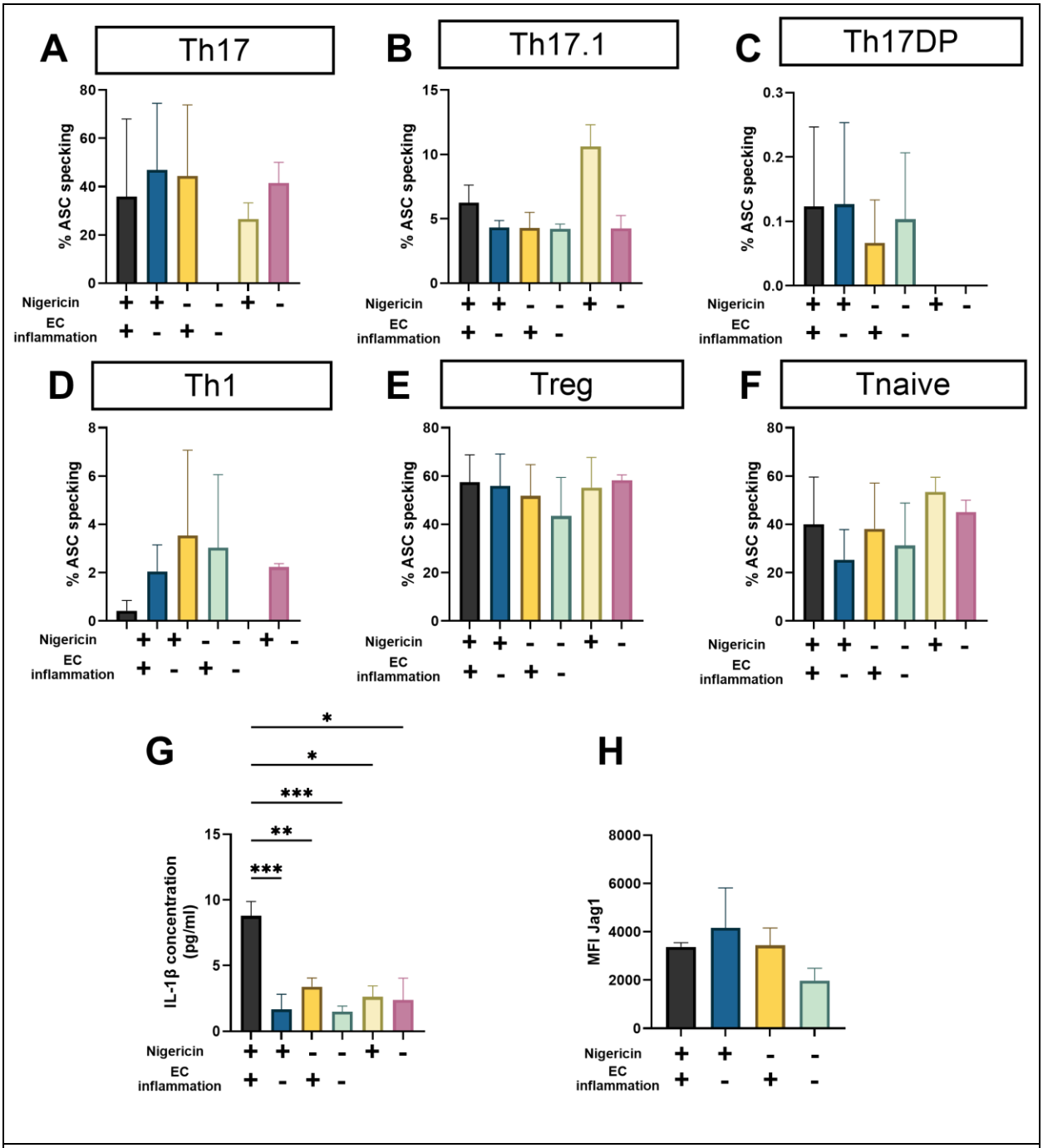

Fig. 3: Contact of nigericin-treated human CD4$^+$ T-cells with inflamed endothelial cells increases IL-1β production. (A-F) Percentage of ASC specking was analysed using flow cytometric analysis in different CD4$^+$ Th subsets (n = 3). T-cells were resting or treated with nigericin for 30 min, and hCMEC/d3 cells were untreated or treated with TNFα and IFNγ for 24h. **(G)** IL-1β protein levels in the supernatant were measured using ELISA (n = 3 **(H)** Jag1 expression was analysed using flow cytometric analysis in hCMEC/d3 cells (n = 3). Statistical analysis was performed using a Kruskal-Wallis test with Dunn's multiple comparisons test (A-F, H) and a one-way ANOVA with a Tukey's multiple comparisons test (G) with *, p<0,05; **, p<0,01; ***, p<0,001. Data are depicted as mean ± SEM. EC, endothelial cell; *ASC, Apoptosis-associated Speck-like protein containing a Caspase recruitment domain; Jag1, Jagged1; MFI, median fluorescence intensity; TNFα, tumour necrosis factor alpha; IFNγ, interferon gamma; IL-1β, interleukin-1β.*

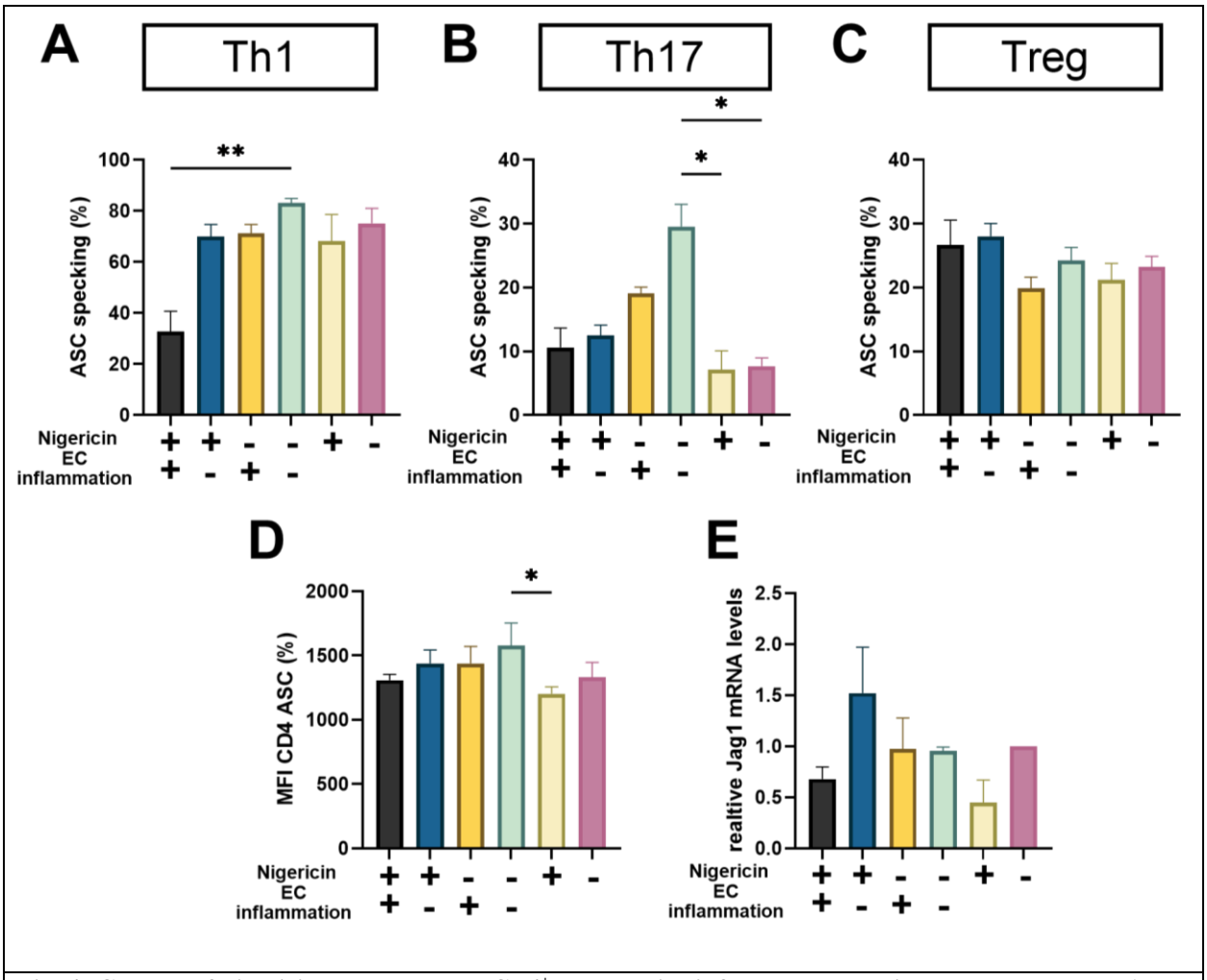

Fig. 4: Contact of nigericin-treated mouse CD4⁺ T-cells with inflamed endothelial cells decreases Th1 and Th17 ASC specking. (A-C) Percentage of ASC specking was analysed using flow cytometric analysis in different CD4⁺ Th subsets. **(D)** MFI of ASC in all CD4⁺ T-cells was analysed using flow cytometric analysis. T-cells were resting or treated with nigericin for 30 min, and mBEND3 cells were untreated or treated with TNFα and IFNγ for 24h (n = 3). **(E)** Jag1 expression was analysed using qPCR in mBEND3 cells (n = 7). Statistical analysis was performed using a Kruskal-Wallis test with Dunn's multiple comparisons test with *, p<0,05; **, p<0,01 (A-E). Data are depicted as mean ± SEM. *EC, endothelial cell; MFI, median fluorescence intensity; ASC, Apoptosis-associated Speck-like protein containing a Caspase recruitment domain; Jag1, Jagged1; TNFα, tumour necrosis factor alpha; IFNγ, interferon gamma.*

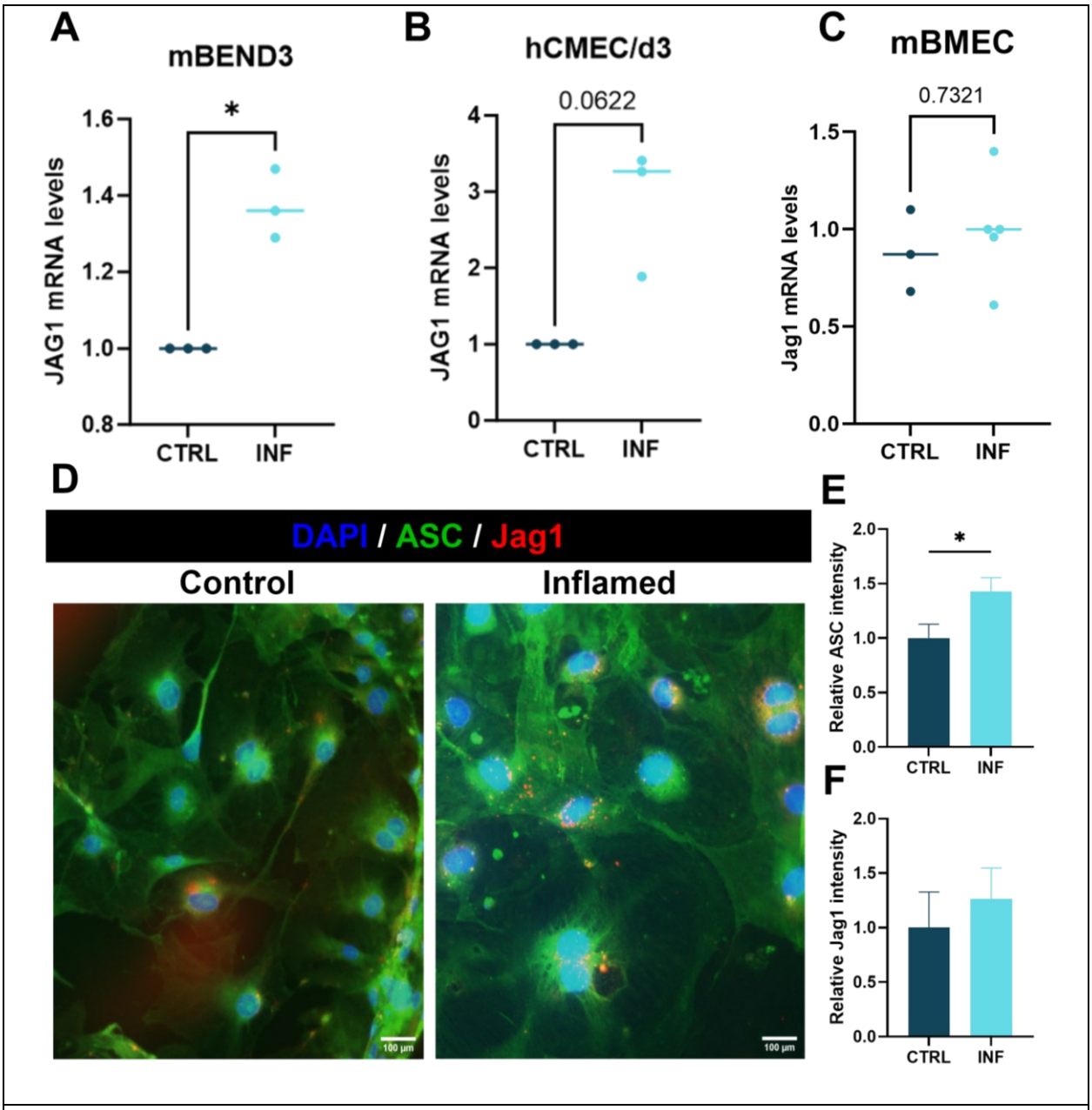

Fig. 5: Inflammation increases Jag1 expression in brain endothelial cells. (A-C) qPCR analysis of Jag1 mRNA expression in mBEND3 cells in fold change (n = 3) **(A)**, hCMEC/d3 cells in fold change (n = 3) **(B)**, and mBMECs (n = 3-5)**(C)**. Cells were untreated or treated with TNFα and IFNγ for 24h. **(D-F)** Representative fluorescence microscopy images **(D)** and quantification of relative mean ASC intensity **(E)** and relative mean Jag1 intensity **(F)** in mBMECs of ASC-GFP mice untreated or treated with TNFα and IFNγ for 48h (n = 4). Immunofluorescence shows ASC (green) and Jag1 (red). Nuclear staining was performed with DAPI (blue). Magnification: 40x objective, 10x ocular. Scale bar 100µm. Statistical analysis was performed using a Mann-Whitney test (A-C) and an unpaired t-test (E-F) with *, $p < 0.05$. Data are depicted as mean ± SEM. *CTRL, control; INF, Inflamed; mBMEC, murine brain microvascular endothelial cells; ASC, Apoptosis-associated Speck-like protein containing a Caspase recruitment domain; Jag1, Jagged1; DAPI 4',6-diamidino-2-phenylindole; TNFα, tumour necrosis factor alpha; IFNγ, interferon gamma.*

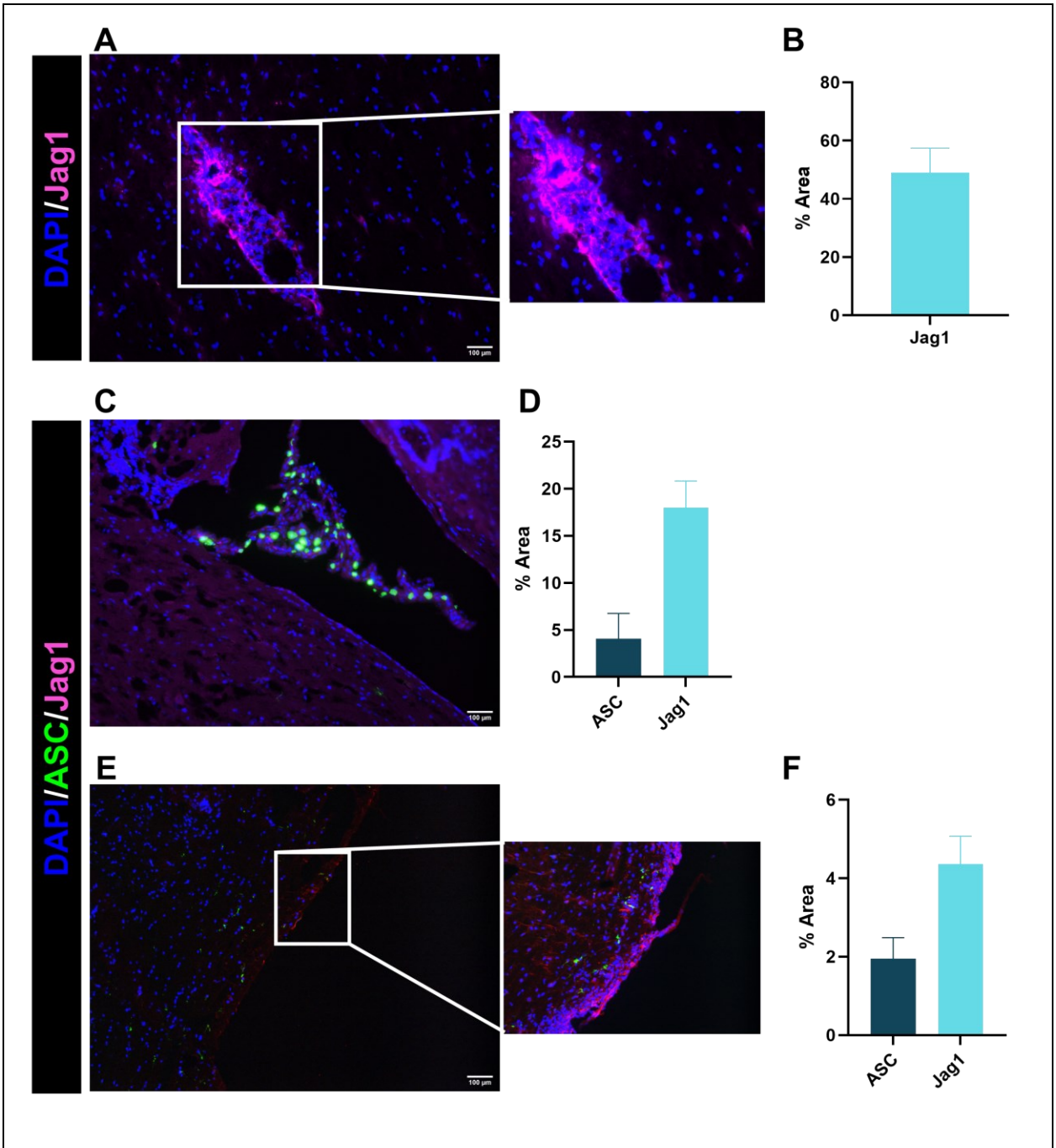

Fig. 6: ASC and Jag1 are expressed in the CNS of MS patients and EAE mice. (A-B) Representative fluorescence microscopy images and quantification of Jag1 expression in active human MS lesions depicted as percentage area (blood vessels: $n = 4$; MS patients: $n = 1$). Immunofluorescence shows Jag1 (magenta). Nuclear staining was performed with DAPI (blue). Magnification: 20x and 40x objective, 10x ocular. **(C-F)** Representative fluorescence microscopy images **(C and E)** and quantification of ASC and Jag1 expression depicted as percentage area **(D and F)** in brains **(C and D)** and spinal cords **(E and F)** of EAE peak mice (brain: $n = 4$, spinal cord: $n = 9$). Immunofluorescence shows ASC (green) and Jag1 (magenta). Nuclear staining was performed with DAPI (blue). Magnification: 10x and 20x objective, 10x ocular. Scale bar 100µm. Statistical analysis was performed using a Spearman r correlation test (D, F). Data are depicted as mean ± SEM. *EAE, experimental autoimmune encephalomyelitis; ASC, Apoptosis-associated Speck-like protein containing a Caspase recruitment domain; Jag1, Jagged1; DAPI 4',6-diamidino-2- phenylindole.*

DISCUSSION

The disruption of the BBB plays a critical role in MS, enabling the migration of myelin-specific T-cells resulting in neuroinflammation. Previous research has explored the link between $CD4^+$ T-cell inflammasome activation and T-cell migration across the BBB (4, 10, 12, 14, 19). To date, however, the exact mechanism behind it remains unclear. Therefore, this study aims to investigate whether inflammasome activation precedes or follows T-cell migration over the BBB.

Previous research demonstrated NLRP3 KO mice are resistant to EAE development, associating the NLRP3 inflammasome with EAE pathogenesis (10, 19, 20). However, the mechanism of how this inflammasome exacerbates EAE remains elusive. Our data now indicate that NLRP3 KO decreases EAE disease severity. Additionally, when comparing Th1/Th17 ratios across the three organs, the ratio was decreased in the lymph nodes and spleen of NLRP3 KO and seemed to increase in the CNS of NLRP3 KO mice compared to WT mice, indicating that especially the Th17 cells could not migrate into the CNS. In line with our results, a study by Inoue *et al.* (2012) also reported that NLRP3 KO mice are resistant to the development of EAE and that both Th17 and Th1 were almost entirely absent in the CNS of these mice (14). However, their results were much more pronounced than ours. Notably, an imbalance of more Th1 and fewer Th17 cells was found across all organs (CNS, spleen, and lymph nodes) in both phenotypes. Similar but more apparent results were also observed in previous research (14).

Since we confirmed that the inflammasome contributes to EAE pathogenesis, potentially through its influence on Th17 cell migration, we explored the possible mechanisms behind this. Activation of inflammasomes all converge into an ASC speck per cell (21). This single supramolecular assembly amplifies inflammasome activation (21, 22). This ASC specking can then be used to assess inflammasome activation, as our results show that ASC specking is significantly decreased when the inflammasome is inhibited by treating PBMCs with MCC950, a specific small-molecule inhibitor that selectively blocks activation of the NLRP3 inflammasome (9, 23). Here, we demonstrate that migration of human PBMCs cells through inflamed ECs increases ASC specking in $CD4^+$ T-cells and thus enhances inflammasome activation. This effect of migration was not seen in PBMCs treated with MCC950, again confirming the involvement of the NLRP3 inflammasome in T-cell migration. These data suggest that inflammasome activation follows T-cell migration over the BBB.

We next investigated whether inflammasome activation could also result from contact with inflamed ECs alone instead of actual migration. Our results show that contact alone with inflamed ECs did not increase ASC specking in any of the human Th subsets. However, IL-1β production does increase when $CD4^+$ T-cells are treated with nigericin and make contact with inflamed ECs. This suggests that a double signal of inflammasome activation together with contact with inflamed ECs might be necessary to enhance IL-1β production. However, it is also possible that the ECs themselves produced the IL-1β (24, 25). It is noteworthy that ICAM, VCAM, and VE-cadherin expression in ECs remained unchanged. This raises the question of whether the concentration of 150 ng/ml rmTNFα and rmIFNγ was sufficient to induce inflammation. Alternatively, it is possible that contact with naïve T-cells had a soothing effect on the ECs, thereby decreasing inflammation. In light of this, it might be a good idea to repeat our co-culture experiments, validate inflammation induction in ECs, and interpret our results with caution.

Furthermore, opposing results were found with mouse $CD4^+$ splenocytes as contact between nigericin-treated Th1 cells with inflamed ECs exhibited significantly reduced ASC speck formation, while resting Th17 co-cultured with control ECs showed significantly higher ASC specking compared to Th17 cells without EC contact. These data suggest that the used dose of 10 μM nigericin was too high and caused cell death in Th1 and Th17 cells that had inflammasome activation. Another explanation could be that the mice used in this experiment were too old, leading to $CD4^+$ T-cells being less responsive, more immunosuppressive, and more prone to cell death (26-28). Since these results contradict those obtained with human cells, it is important to note some differences between the two co-culture setups. Human $CD4^+$ T-cells were isolated from whole blood, whereas mouse $CD4^+$ T-cells were isolated from the spleen. Splenic $CD4^+$ T-cells are often in a more activated state, while $CD4^+$ T-cells in the blood are typically in a resting or naïve state

(8). Additionally, only $CD4^+$ memory T-cells were isolated from human PBMCs. Research by Beynon *et al.* (2012) has shown that human $CD4^+$ memory T-cells are differently regulated than those in mice. Mouse $CD4^+$ memory T-cells suppress inflammasome activation by mechanisms dependent on ligands of the TNFR family (29). In contrast, human $CD4^+$ memory T-cells must first be primed with IFNβ to affect NLRP3 inflammasome activation (30). However, both studies reported indirect effects on inflammasome activation. To exclude differences resulting from the use of different subsets, future experiments should use the same subsets for both human and mouse co-cultures. Additionally, future research should determine the optimal dose of nigericin and repeat this study using spleens isolated from younger mice.

Given that IL-1β production increased upon direct contact of human $CD4^+$ T-cells with inflamed ECs, we investigated whether Jag1 could be the responsible trigger for this phenomenon. Our findings demonstrate that inflammation in BBB ECs is associated with upregulated Jag1 gene expression. This observation supports the hypothesis that increased Jag1 on BBB ECs triggers the increase in $CD4^+$ T-cell inflammasome activation seen during *in vitro* migration and enhances IL-1β production seen upon contact with inflamed ECs.

Building on this hypothesis, we explored the potential involvement of Jag1 in MS and EAE pathogenesis. Here, we demonstrate that Jag1 is expressed in active MS lesions, especially around the blood vessels, supporting our results that migration over the BBB results in inflammasome activation. Similarly, ASC-GFP mice induced with EAE exhibited concurrent expression of ASC and Jag1 at the disease peak in both brain and spinal cord tissues. The ASC signal was primarily localised around the choroid plexus and blood vessels in the brain, which is interesting since Th17 cells reach the CNS initially via the choroid plexus to initiate EAE (31). Remarkably, in the spinal cord, both ASC and Jag1 expression was more evident at tissue margins, which could also be associated with migration across the blood-spinal cord barrier at the periphery of the spinal cord.

Since Jag1 is expressed in active MS lesions and both ASC and Jag1 are expressed in the CNS of EAE mice, we aimed to further assess the presence of inflammasome activation by exploring the presence of IL-1β in the brains of MS patients. Our results indicate that IL-1β expression was evident in active MS lesions. This is consistent with earlier studies by Burm *et al.* (2016) (32) and Kawana *et al.* (2013) (33), which described the characterisation of IL-1β in active lesions. Furthermore, this corresponds with the increase in IL-1β production observed upon contact between nigericin-treated $CD4^+$ T-cells and inflamed ECs described in this study. However, it is important to note that the observed IL-1β expression is not necessarily a direct result of $CD4^+$ T-cell inflammasome activation, as various cell types – including monocytes, macrophages, astrocytes, and brain endothelial cells – can produce IL-1β, and this production can even occur independently of inflammasomes (24, 34-37).

Future research should aim to validate our findings through repeated co-culture experiments to ensure proper induction of inflammation in ECs. These experiments should also use the same human and mouse $CD4^+$ Th subsets, given the differing results observed with mouse $CD4^+$ splenocytes. Moreover, since we have demonstrated that IL-1β is present in active MS lesions, further research should focus on co-localising IL-1β, ASC, and CD4 to provide a complete picture of $CD4^+$ T-cell intrinsic inflammasome activation in MS. Furthermore, the potential involvement of Jag1 in $CD4^+$ T-cell inflammasome activation during BBB migration warrants further exploration, particularly in the context of MS and EAE pathogenesis. It is also essential to examine and acknowledge the indirect effect of inflammasome activation on $CD4^+$ T-cells in the pathogenesis of MS and EAE.

Collectively, we show that the $CD4^+$ T-cell migration across brain ECs results in inflammasome activation in these cells, possibly due to the increased expression of Jag1 on inflamed brain ECs. Additionally, we demonstrate that the NLRP3 inflammasome plays a role in Th17 cell migration into the CNS during EAE development. Nevertheless, more research is warranted to fully understand how inflammasome activation contributes to MS and how these results can be translated into new possibilities in treatment development.

CONCLUSION

In this research paper, we investigated whether inflammasome activation precedes or follows T-cell migration over the BBB and elucidated the *in vitro* and *in vivo* interplay of inflammasome activation and $CD4^+$ T-cells. First, we show that the NLRP3 inflammasome plays a role in Th17 cell migration into the CNS during EAE development. Additionally, we found that $CD4^+$ T-cell migration across brain ECs results in inflammasome activation, possibly due to the increased expression of Jag1 on inflamed brain ECs. Lastly, our data indicate that Jag1 and IL- 1β are expressed in active MS lesions, and both ASC and Jag1 are expressed in the CNS of EAE mice. In the context of MS, these findings could benefit the search for novel therapeutic approaches and the unravelling of the pathophysiological mechanism of this disease. However, further research should explore the exact mechanisms of how $CD4^+$ T-cell inflammasome activation adds to MS.

REFERENCES

1. (2020) Atlas of MS MS International Federation,
2. Tafti, D., Ehsan, M., andXixis, K. L. (2022) Multiple Sclerosis In StatPearls, Treasure Island (FL)
3. Correale, J., Gaitan, M. I., Ysrraelit, M. C., andFiol, M. P. (2017) Progressive multiple sclerosis: from pathogenic mechanisms to treatment Brain **140**, 527-546 10.1093/brain/aww258
4. Braga, T. T., Brandao, W. N., Azevedo, H., Terra, F. F., Melo, A. C. L., Pereira, F. V. *et al.* (2019) NLRP3 gain-of-function in CD4(+) T lymphocytes ameliorates experimental autoimmune encephalomyelitis Clin Sci (Lond) **133**, 1901-1916 10.1042/CS20190506
5. Marchetti, L., andEngelhardt, B. (2020) Immune cell trafficking across the blood-brain barrier in the absence and presence of neuroinflammation Vasc Biol **2**, H1-H18 10.1530/VB-19-0033
6. Evavold, C. L., andKagan, J. C. (2018) How Inflammasomes Inform Adaptive Immunity J Mol Biol **430**, 217-237 10.1016/j.jmb.2017.09.019
7. Kemper, C., Chan, A. C., Green, J. M., Brett, K. A., Murphy, K. M., andAtkinson, J. P. (2003) Activation of human CD4+ cells with CD3 and CD46 induces a T-regulatory cell 1 phenotype Nature **421**, 388-392 10.1038/nature01315
8. Abul K. Abbas, A. H. L., Shiv Pillai (2019) *Basic Immunology*, SIXTH EDITION Ed., Elsevier Inc., Philadelphia
9. Tweedell, R. E., andKanneganti, T. D. (2020) Advances in Inflammasome Research: Recent Breakthroughs and Future Hurdles Trends Mol Med **26**, 969-971 10.1016/j.molmed.2020.07.010
10. Gris, D., Ye, Z., Iocca, H. A., Wen, H., Craven, R. R., Gris, P. *et al.* (2010) NLRP3 plays a critical role in the development of experimental autoimmune encephalomyelitis by mediating Th1 and Th17 responses J Immunol **185**, 974-981 10.4049/jimmunol.0904145
11. Brydges, S. D., Mueller, J. L., McGeough, M. D., Pena, C. A., Misaghi, A., Gandhi, C. *et al.* (2009) Inflammasome-mediated disease animal models reveal roles for innate but not adaptive immunity Immunity **30**, 875-887 10.1016/j.immuni.2009.05.005
12. Martin, B. N., Wang, C., Zhang, C. J., Kang, Z., Gulen, M. F., Zepp, J. A. *et al.* (2016) T cell-intrinsic ASC critically promotes T(H)17-mediated experimental autoimmune encephalomyelitis Nat Immunol **17**, 583-592 10.1038/ni.3389
13. Le Friec, G., Sheppard, D., Whiteman, P., Karsten, C. M., Shamoun, S. A., Laing, A. *et al.* (2012) The CD46-Jagged1 interaction is critical for human TH1 immunity Nat Immunol **13**, 1213-1221 10.1038/ni.2454
14. Inoue, M., Williams, K. L., Gunn, M. D., andShinohara, M. L. (2012) NLRP3 inflammasome induces chemotactic immune cell migration to the CNS in experimental autoimmune encephalomyelitis Proc Natl Acad Sci U S A **109**, 10480-10485 10.1073/pnas.1201836109
15. Hermans, D., Houben, E., Baeten, P., Slaets, H., Janssens, K., Hoeks, C. *et al.* (2022) Oncostatin M triggers brain inflammation by compromising blood-brain barrier integrity Acta Neuropathol

144, 259-281 10.1007/s00401-022-02445-0

16. Hosseinkhani, B., Duran, G., Hoeks, C., Hermans, D., Schepers, M., Baeten, P. *et al.* (2023) Cerebral microvascular endothelial cell-derived extracellular vesicles regulate blood - brain barrier function Fluids Barriers CNS **20**, 95 10.1186/s12987-023-00504-6
17. Grajchen, E., Loix, M., Baeten, P., Corte-Real, B. F., Hamad, I., Vanherle, S. *et al.* (2023) Fatty acid desaturation by stearoyl-CoA desaturase-1 controls regulatory T cell differentiation and autoimmunity Cell Mol Immunol **20**, 666-679 10.1038/s41423-023-01011-2
18. Baeten, P., Hamad, I., Hoeks, C., Hiltensperger, M., Van Wijmeersch, B., Popescu, V. *et al.* (2024) Rapamycin rescues loss of function in blood-brain barrier-interacting Tregs JCI Insight **9**, 10.1172/jci.insight.167457
19. Inoue, M., Williams, K. L., Oliver, T., Vandenabeele, P., Rajan, J. V., Miao, E. A. *et al.* (2012) Interferon-beta therapy against EAE is effective only when development of the disease depends on the NLRP3 inflammasome Sci Signal **5**, ra38 10.1126/scisignal.2002767
20. Jha, S., Srivastava, S. Y., Brickey, W. J., Iocca, H., Toews, A., Morrison, J. P. *et al.* (2010) The inflammasome sensor, NLRP3, regulates CNS inflammation and demyelination via caspase-1 and interleukin-18 J Neurosci **30**, 15811-15820 10.1523/JNEUROSCI.4088-10.2010
21. Govindarajan, V., de Rivero Vaccari, J. P., andKeane, R. W. (2020) Role of inflammasomes in multiple sclerosis and their potential as therapeutic targets J Neuroinflammation **17**, 260 10.1186/s12974-020-01944-9
22. Sharma, D., andKanneganti, T. D. (2016) The cell biology of inflammasomes: Mechanisms of inflammasome activation and regulation J Cell Biol **213**, 617-629 10.1083/jcb.201602089
23. Perregaux, D. G., McNiff, P., Laliberte, R., Hawryluk, N., Peurano, H., Stam, E. *et al.* (2001) Identification and characterization of a novel class of interleukin-1 post-translational processing inhibitors J Pharmacol Exp Ther **299**, 187-197, https://www.ncbi.nlm.nih.gov/pubmed/11561079
24. Heidary, M., Rakhshi, N., Pahlevan Kakhki, M., Behmanesh, M., Sanati, M. H., Sanadgol, N. *et al.* (2014) The analysis of correlation between IL-1B gene expression and genotyping in multiple sclerosis patients J Neurol Sci **343**, 41-45 10.1016/j.jns.2014.05.013
25. de Jong, B. A., Huizinga, T. W., Bollen, E. L., Uitdehaag, B. M., Bosma, G. P., van Buchem, M. A. *et al.* (2002) Production of IL-1beta and IL-1Ra as risk factors for susceptibility and progression of relapse-onset multiple sclerosis J Neuroimmunol **126**, 172-179 10.1016/s0165-5728(02)00056-5
26. Schwab, R., Szabo, P., Manavalan, J. S., Weksler, M. E., Posnett, D. N., Pannetier, C. *et al.* (1997) Expanded CD4+ and CD8+ T cell clones in elderly humans J Immunol **158**, 4493-4499, https://www.ncbi.nlm.nih.gov/pubmed/9127016
27. van Deursen, J. M. (2014) The role of senescent cells in ageing Nature **509**, 439-446 10.1038/nature13193
28. Thomas, A. L., Godarova, A., Wayman, J. A., Miraldi, E. R., Hildeman, D. A., andChougnet, C. A. (2023) Accumulation of immune-suppressive CD4 + T cells in aging - tempering inflammaging at the expense of immunity Semin Immunol **70**, 101836 10.1016/j.smim.2023.101836
29. Guarda, G., Dostert, C., Staehli, F., Cabalzar, K., Castillo, R., Tardivel, A. *et al.* (2009) T cells dampen innate immune responses through inhibition of NLRP1 and NLRP3 inflammasomes Nature **460**, 269-273 10.1038/nature08100
30. Beynon, V., Quintana, F. J., andWeiner, H. L. (2012) Activated human CD4+CD45RO+ memory T-cells indirectly inhibit NLRP3 inflammasome activation through downregulation of P2X7R signalling PLoS One **7**, e39576 10.1371/journal.pone.0039576
31. Reboldi, A., Coisne, C., Baumjohann, D., Benvenuto, F., Bottinelli, D., Lira, S. *et al.*

(2009) C-C chemokine receptor 6-regulated entry of TH-17 cells into the CNS through the choroid plexus is required for the initiation of EAE Nat Immunol **10**, 514-523 10.1038/ni.1716

32. Burm, S. M., Peferoen, L. A., Zuiderwijk-Sick, E. A., Haanstra, K. G., t Hart, B. A., van der Valk, P. *et al.* (2016) Expression of IL-1beta in rhesus EAE and MS lesions is mainly induced in the CNS itself J Neuroinflammation **13**, 138 10.1186/s12974-016-0605-8
33. Kawana, N., Yamamoto, Y., Ishida, T., Saito, Y., Konno, H., Arima, K. *et al.* (2013) Reactive astrocytes and perivascular macrophages express NLRP3inflammasome in active demyelinating lesions of multiple sclerosisand necrotic lesions of neuromyelitis optica and cerebral infarction Clinical and Experimental Neuroimmunology **4**, i, 247-363 10.1111/cen3.12068
34. Lukens, J. R., Gross, J. M., Calabrese, C., Iwakura, Y., Lamkanfi, M., Vogel, P. *et al.* (2014) Critical role for inflammasome-independent IL-1beta production in osteomyelitis Proc Natl Acad Sci U S A **111**, 1066-1071 10.1073/pnas.1318688111
35. Provoost, S., Maes, T., Pauwels, N. S., Vanden Berghe, T., Vandenabeele, P., Lambrecht, B. N. *et al.* (2011) NLRP3/caspase-1-independent IL-1beta production mediates diesel exhaust particle-induced pulmonary inflammation J Immunol **187**, 3331-3337 10.4049/jimmunol.1004062
36. Bauer, J., Berkenbosch, F., Van Dam, A. M., andDijkstra, C. D. (1993) Demonstration of interleukin-1 beta in Lewis rat brain during experimental allergic encephalomyelitis by immunocytochemistry at the light and ultrastructural level J Neuroimmunol **48**, 13-21 10.1016/0165-5728(93)90053-2
37. Christy, A. L., Walker, M. E., Hessner, M. J., andBrown, M. A. (2013) Mast cell activation and neutrophil recruitment promotes early and robust inflammation in the meninges in EAE J Autoimmun **42**, 50-61 10.1016/j.jaut.2012.11.003

This text was grammatically refined by GenAI.

Acknowledgements – I would like to express my gratitude to my daily supervisor, Gayel Duran, and my promotor, Prof. Dr. Bieke Broux, for their invaluable feedback, consistent support, and guidance throughout my senior internship and writing this paper. Their scientific and practical insights have been instrumental. I also wish to thank fellow CBN team members and my second examiner, Prof. Dr. Jeroen Bogie, for their skilful assistance and ongoing feedback. Additionally, I appreciate the support and input from other members of the Biomedical Research Institute at Hasselt University.

Author contributions – Prof. Dr. Bieke Broux and Gayel Duran conceived and designed the research. Joke Aerts and Gayel Duran performed experiments and data analysis. All authors discussed the results. Joke Aerts wrote the manuscript. Gayel Duran carefully revised and edited the manuscript.

SUPPORTING INFORMATION

Supplementary methods

Human brain-derived endothelial cells – The human cerebral microvascular endothelial cell line hCMEC/d3 was provided by Tebu-bio (Le Perray-en-Yvelines) and cultured as previously described (15, 16). Briefly, the cells were cultured using the EGM™-2 MV Microvascular Endothelial Cell Growth Medium-2 BulletKit™ (CC-3202, Lonza), in 75 µg/ml collagen type I (Merck) coated plates or inserts (Greiner). When 80% confluent, medium was changed to EBM™-2 Basal Medium (CC-3156, Lonza) supplemented with 1 ng/ml human fibroblast growth factor (FGF), 1.4 µM hydrocortisone, 10 µg/ml gentamicin, 1 µg/ml amphotericin (A2942, all Merck), and 2.5% FCS (Gibco™, Thermo Fisher Scientific). When starting experiments, medium was changed to EBM™-2 Basal Medium supplemented with 1 ng/ml human FGF, 10 µg/ml gentamicin, 1 µg/ml amphotericin, and 0.25% FCS. Inflammation was induced by treatment with 100 ng/ml rhTNFα and 10 ng/ml rhIFNγ (Peprotech) for 24h.

RNA isolation, cDNA synthesis, and qPCR – For quantitative polymerase chain reaction (qPCR), cells were collected by scraping in RLT buffer containing 1% β-mercapto-ethanol. RNA was isolated from cells using the RNeasy Mini Kit (74106, QIAGEN), following the manufacturer's instructions. Purity and concentrations were determined using the Spectrophotometer ND-1000 (NanoDrop®). Isolated RNA was converted to cDNA using the qScript cDNA synthesis kit (95048 500; Quanta Biosciences) according to the manufacturer's instructions, and qPCR was performed with primers (Table S3) for the genes of interest. Data as ΔΔCt was normalised to the two most stable housekeeping genes.

Immunohistochemistry – Murine brain and spinal cord tissue were cut into 10 µm serial sections using the Leica CM3050S cryostat (Leica Microsystems). The sections were post-fixed with frozen acetone for 10 min, followed by three washes with PBS. Sections were then blocked with the 50% Dako protein blocking buffer (DAKO) in 0.5% Triton-PBS for 30 minutes at room temperature. Next, sections were incubated overnight with rabbit-anti-jagged1 (1:100, PA5-86057, Invitrogen) as primary antibody at 4 °C. Immunoreactivity was visualised using goat anti-rabbit Alexa Fluor 555 (1/250, Invitrogen™, Thermo Fisher Scientific) after 1h incubation at room temperature. Nuclear staining was performed with 4',6-diamidino 2-phenylindole (DAPI). Finally, sections were incubated with 0.3% Sudan Black (Merck) in 70% ethanol to limit autofluorescence and mounted with Fluoromount-G™ Mounting Medium (Invitrogen™, Thermo Fisher Scientific). Microscopic analysis was performed using Leica DM2000 LED and Leica Application Suite X (LAS X) software (Leica Microsystems).

Supplementary tables and figures

Table S1: Overview of healthy whole blood donors.

Donor Type	Donor ID	Experiment
HD	BM2-944	Human migration assay
HD	BM2-945	Human migration assay
HD	BM2-951	Human co-culture
HD	BM2-978	Human migration assay
HD	BM2-979	Human migration assay
HD	BM2-983	Human co-culture
HD	BM2-984	Human co-culture

HD, healthy donor.

Table S2: Antibodies for flow cytometry.

Marker	Catalogue number	Supplier
CD16 – FITC (human)	302005	BioLegend
CD14 – BV605 (human)	301833	BioLegend
CD8 – BV711 (human)	344733	BioLegend
CD19 – BV785 (human)	363027	BioLegend
CD4 – APC-Fire750 (human)	300559	BioLegend
CD27 – BV606 (human)	302829	BioLegend
CD25 – BV711 (human)	302635	BioLegend
CCR4 – APC-Fire810 (human)	359439	BioLegend
CD57 – BV785 (human)	393329	BioLegend
CCR6 – PerCP/Cy5.5 (human)	353405	BioLegend
CD28 – PE-Cy5 (human)	302925	BioLegend
CXCR3 – BV421 (human)	353719	BioLegend
CD46 – PE/Dazzle™ 594 (human)	362543	BioLegend
IL-1β – Pacific Blue (human)	511710	BioLegend
ASC – PE (human)	65904	BioLegend
FOXP3 – AF647 (human)	320113	BioLegend
CD3 – BV605 (Mouse)	100237	BioLegend
CD19 – BV650 (mouse)	115541	BioLegend
CD4 – Pacific Blue (mouse)	100428	BioLegend
CD8a – BV510 (mouse)	100751	BioLegend
CD45 – AF700 (mouse)	103128	BioLegend
CD11b – PerCP/Cy5.5 (mouse)	101228	BioLegend
Ly-6C –BV785 (mouse)	128041	BioLegend

CXCR3 – PE (mouse)	126506	BioLegend
CCR6 – PE-Cy7 (mouse)	129815	BioLegend
CD25 – APC (mouse)	102012	BioLegend

Table S3: Primer Sequences.

Target gene	Forward primer (5'-3')	Reverse primer (5'-3')
Jag1 (mouse)	5'-ATG ATG GGA AAG GGG TTA GG-3'	5'-TGT GAT CTG GCC ACA AAG AG-3'
TBP* (mouse)	5'-ATG GTG TGC ACA GGA GCC AAG-3'	5'-TCA TAG CTA CTG AAC TGC TG-3'
YWHAZ* (mouse)	5'-GCA ACG ATG TAC TGT CTC TTT TGG-3'	5-GTC CAC AAT TCC TTT CTT GTC ATC-3'
HMBS* (mouse)	5'-GAT GGG CAA CTG TAC CTG ACT G-3'	5'-CTG GGC TCC TCT TGG AAT G-3'

*Housekeeping genes

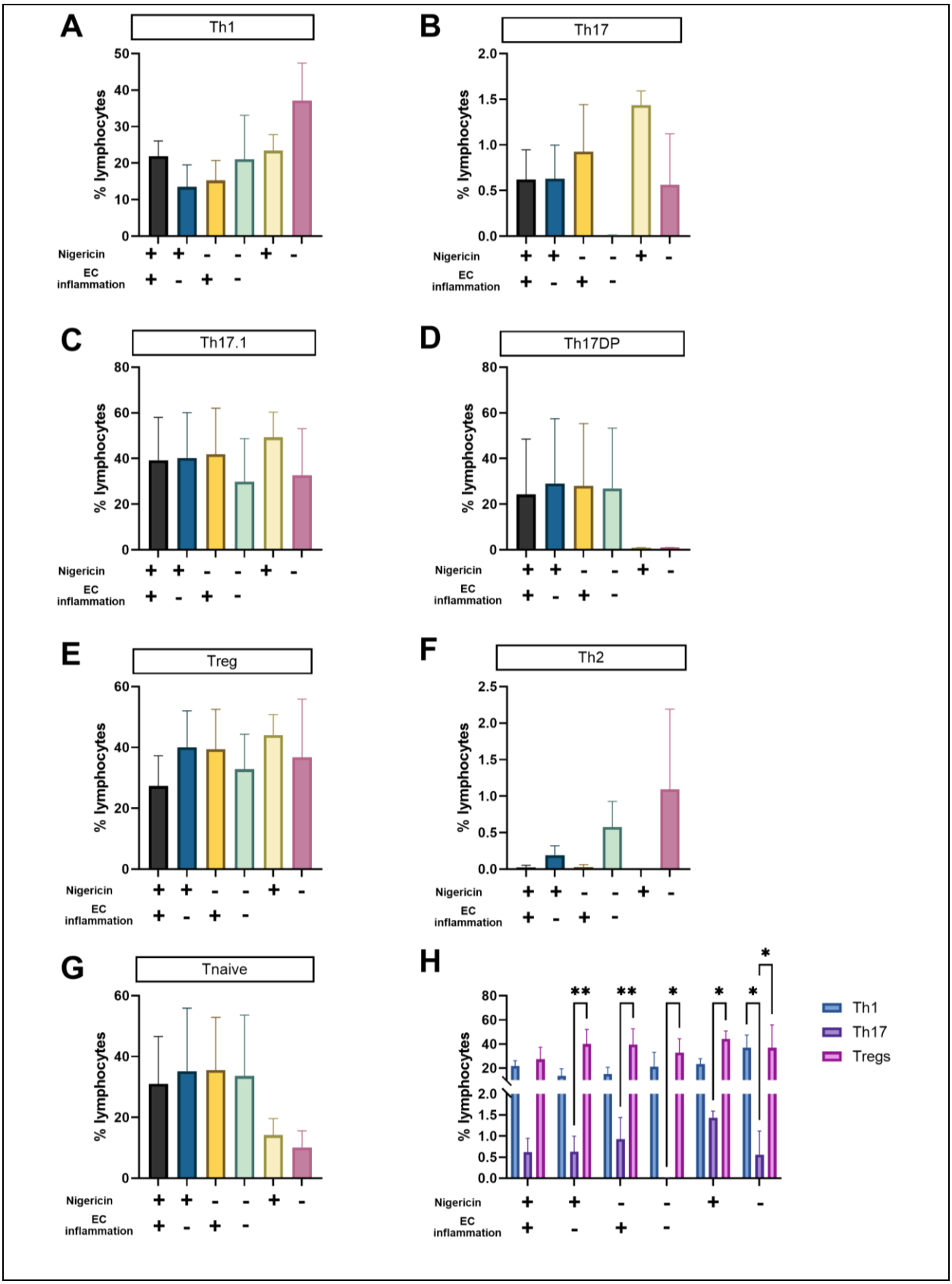
A
Th1
% lymphocytes
Nigericin
EC inflammation
B
Th17
C
Th17.1
D
Th17DP
E
Treg
F
Th2
G
Tnaive
H
Th1
Th17
Tregs

Fig. S1: Nigericin-treated T-cells in contact with inflamed ECs decreased the number of Tregs. Percentages of Th1 **(A)**, Th17 **(B)**, Th17.1 **(C)**, Th17DP **(D)**, Treg **(E)**, Th2 **(F)**, and Tnaive **(G)** cells were analysed using flow cytometric analysis, and Th1, Th17, and Treg subset were compared to each other **(H)**. T-cells were resting or treated with nigericin for 30 min, and hCMEC/d3 cells were untreated or treated with TNFα and IFNγ for 24h (n = 3). Statistical analysis was performed using a Kruskal-Wallis test with Dunn's multiple comparisons test (A-G) and a two-way ANOVA with a Bonferroni's multiple comparisons test with *, p<0,05; **, p<0,01 (H). Data are depicted as mean ± SEM. *EC, endothelial cell; TNFα, tumour necrosis factor alpha; IFNγ, interferon gamma; IL-1β, interleukin-1β.*

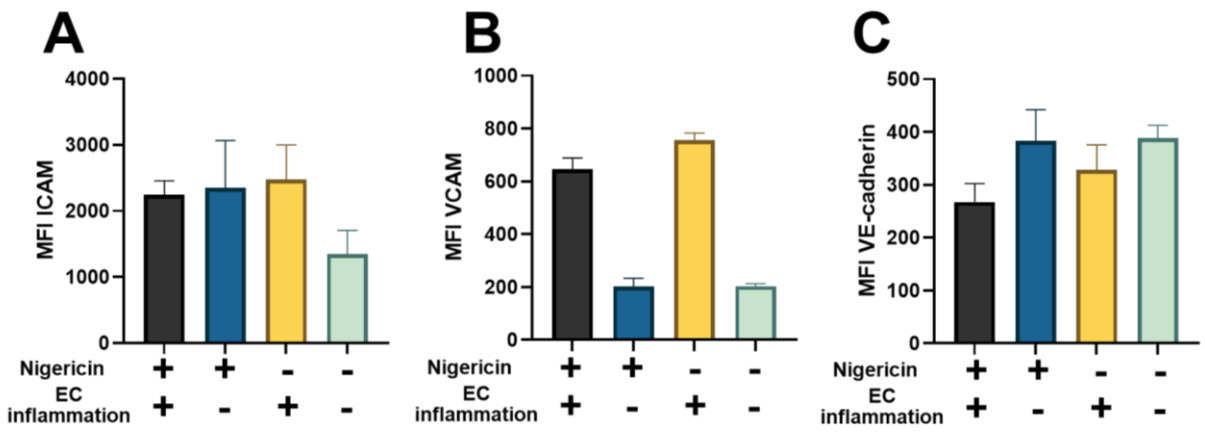

Fig. S2: Contact of human CD4$^+$ T-cells with endothelial cells does not affect ICAM, VCAM, and VE-cadherin expression. ICAM **(A)**, VCAM **(B)**, and VE-Cadherin **(C)** expressions were analysed using flow cytometric analysis in hCMEC/d3 cells (n = 3). T-cells were resting or treated with nigericin for 30 min, and hCMEC/d3 cells were untreated or treated with TNFα and IFNγ for 24h. Statistical analysis was performed using a Kruskal-Wallis test with Dunn's multiple comparisons test (A-C). Data are depicted as mean ± SEM. EC, endothelial cell*; MFI, median fluorescence intensity; TNFα, tumour necrosis factor alpha; IFNγ, interferon gamma; IL-1β, interleukin-1β.*

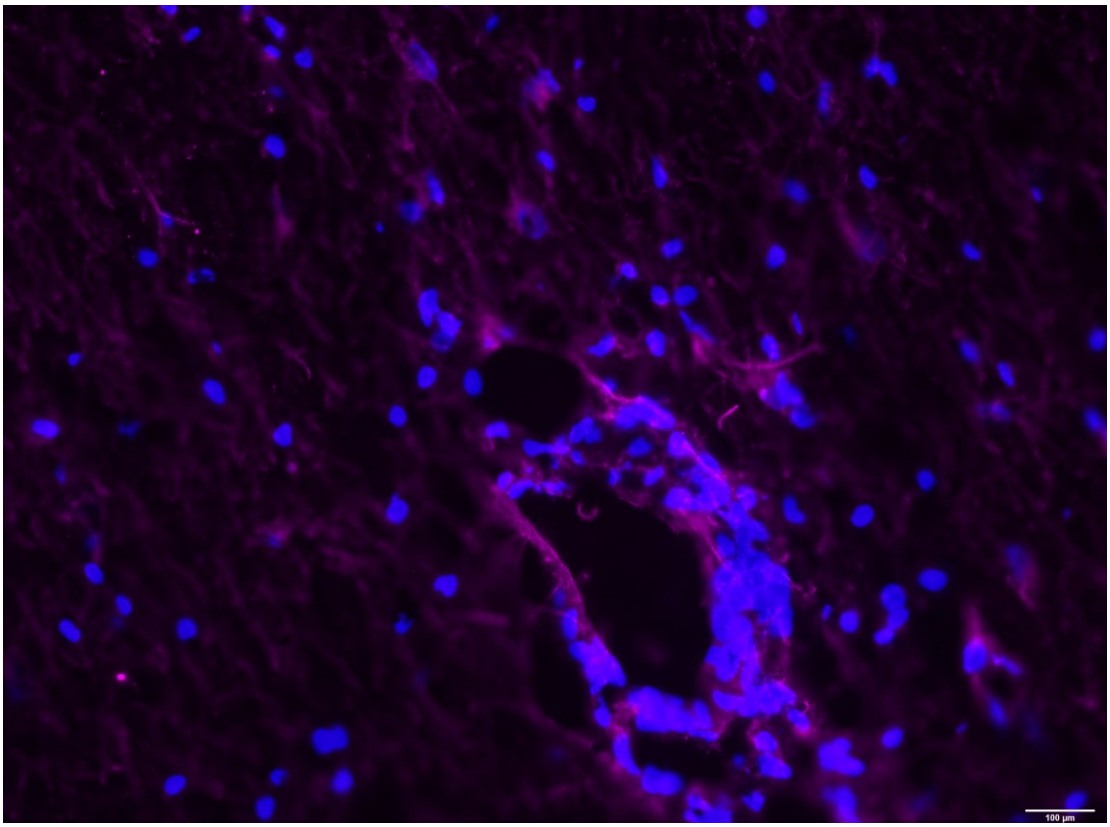

Fig. S3: IL-1β expression in the brains of MS patients. Representative fluorescence microscopy image of IL-1β expression in active human MS lesions (n = 1). Immunofluorescence shows Jag1 (magenta). Nuclear staining was performed with DAPI (blue). Magnification: 40x objective, 10x ocular. Scale bar 100µm. *Jag1, Jagged1; DAPI 4',6-diamidino-2-phenylindole*.